

# Microwave-assisted hydrothermal synthesis of Cu-doped titanate nanotubes: photoluminescence and photocatalysis properties.

D. C. Manfroi\*, L. P. Andrade\*\*, A. A. Cavaleiro\*\*\*, A. dos Anjos\*\*\*, G. F. Teixeira\*, L. A. Perazolli\*, J. A. Varela\*, M. A. Zaghete\*

\* Chemistry Institute, UNESP, Araraquara, SP, Brazil, danimanfroi@hotmail.com; guigui\_iq@hotmail.com; leiningp@iq.unesp.br; varela@iq.unesp.br; zaghete@iq.unesp.br.

\*\* Centro Universitário de Araraquara, SP, Brazil, lidiane.pand@gmail.com.

\*\*\* UEMS, Naviraí, MS, Brazil, albecava@uems.br; piu\_floripa@uems.br.

## ABSTRACT

The synthesis of Cu-doped nanotubes was successfully realized using the hydrothermal method assisted by microwave (MWH). The structure found from XRD shows a typical profile of the layered titanate, containing no peak for secondary phases and no copper phase. These titanates have nanotubes morphology, independent of the synthesis time is 2 or 4 hours. From EDS analysis is possible to verify both the copper and sodium presence, indicating the intercalations between  $\text{Na}^+$  and  $\text{Cu}^{2+}$  ions on the structure. The photoluminescence analysis indicated that the CuNT-4h sample have more surface defects and lower rate of electron-hole recombination. The presence of these particular types of defects leads to enhanced photocatalytic activity of CuNT-4h sample relative to the other. This study concluded that the Cu-doped nanotubes have higher photocatalytic activity than the  $\text{TiO}_2$ -anatase (synthesis precursor) and their activity depends on the type of defects present in the sample.

**Keywords:** Cu-doped nanotubes, microwave hydrothermal method, layered titanates, photoluminescence, photocatalysis.

## 1 INTRODUCTION

The formation of titanate nanotubes from  $\text{TiO}_2$  powder by simple hydrothermal methods was first demonstrated by Kasuga et al. [1, 2]. This kind of method is based on hydrothermal treatment of  $\text{TiO}_2$  powders in aqueous NaOH solutions, at lowers temperatures and under pressure [3, 4]. The heat treatment can be conventional [1, 2] or by microwave [5, 6]. Its accepted that sodium titanates in morphologie of nanotubes or nanoribbons are of layered trititanate structure characterized by a typical interlayer distance of  $\sim 0.9$  nm [7]. Since then, alkali titanates have been intensively investigated mostly because of their properties [3] especially as good candidates for organic photomineralization [8].

The interest for metal transition doping of 1D titanate nanostructures is enormous. Both 1D structure pure NaTiNRs (nanorods) and  $\text{Cu}^{2+}$  impregnated on NaTiNTs (nanotubes) has shown to catalyze decomposition of  $\text{NO}_{2(g)}$

and  $\text{NO}_{(g)}$  [7]. The changed surface chemistry of doped titanate nanostructures is a key factor for enhanced catalytic, photocatalytic, or gas-sensing properties, to mention only few possibilities [7]. Some research has focused on doping of titanate nanotubes (with elements such as carbon, nitrogen or tungsten) and this might further enhance the photocatalytic efficiencies of the nanotube materials by extending the absorption onset into the visible light region [9].

The photoluminescence (PL) spectrum can be useful to study energy levels and it's strongly dependent on the surface condition, and hence information on surface properties can be obtained by PL spectroscopy which is very important for photocatalysis applications.[10]

In the present work we report the synthesis of Cu-doped titanate nanotubes (CuNT) by microwave-assisted hydrothermal method (MWH).  $\text{TiO}_2$  anatase was used as a precursor and  $\text{Cu}^{2+}$  as dopant, the structural, photoluminescence and photocatalytic properties were studied.

## 2 EXPERIMENTAL

Copper doped titanate nanotubes were successfully synthesized using MWH. The Flowchart in Fig. 1 shows a schematic of the synthesis steps used in this study. The raw material  $\text{TiO}_2$  was added into 50 mL of 10 M NaOH in a Teflon container. Then 5% w/w of  $\text{Cu}^{2+}$  was added to vessel, and the reaction was promulgated at 450 W, 130 °C for 2 h (CuNT-2h) and 4 h (CuNT-4h) in a microwave digestion system (MARS-5), and cooled to room temperature. The powder samples obtained were washed with deionized water until the pH was stabilized to about 6.0 and were then dried at room temperature.

All of the samples were morphologically and structurally characterized by X-ray diffractometry (XRD), scanning electron microscopy (SEM). For the XRD technique, a Rigaku 2000 diffractometer with monochromatic Cu K $\alpha$  radiation at  $2\theta$  range of 10-80° with step of 0.01° was used. The particles morphology was investigated by SEM equipped with EDS detector on a JEOL FEG-SEM, JSM-7500F. The photoluminescence spectra were collected through a Thermal Jarrel-Ash monochromator Monospec 27 and a Hamamatsu R446

photomultiplier, with wavelength of 350 nm for excitation of krypton laser ions (Coherent Innova) with power maintained at 550 mW.

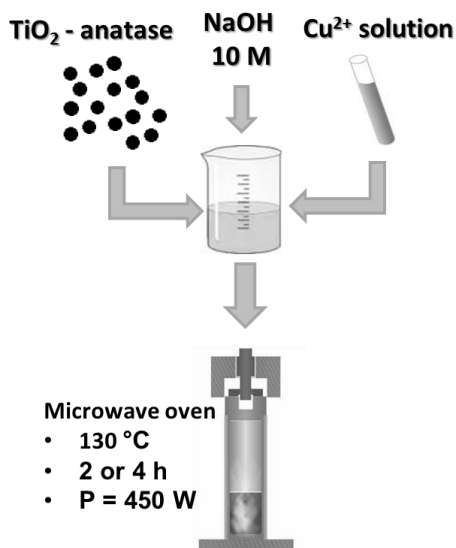


**Figure 1** – Flowchart for synthesis of CuNT for 2 and 4 hours.

Photocatalytic studies were carried out using  $100\text{ mg}\cdot\text{L}^{-1}$  of  $\text{TiO}_2$ -anatase and nanotubes sample dispersed in  $500\text{ mL}$  of  $0.01\text{ mmol}\cdot\text{L}^{-1}$  aqueous solution of rhodamine-B (RB). The suspended solution was stirred a few minutes in the dark and then it was put under a Phillips germicide lamp (254 nm). Degradation was monitored by taking aliquots at increasing time intervals. These aliquots were filtered with Millipore<sup>®</sup> membranes ( $0.45\ \mu\text{m}$ ) and then tested using a UV-Vis Femto Cirrus 80 PR spectrometer to get the absorption spectra. The concentration curve was obtained by maximum RB absorbance peak (554 nm). The rate of degradation was obtained according to (1):

$$\ln\left(\frac{A_0}{A}\right) = kt \quad (1)$$

Where  $A_0$  is the initial absorbance, namely, after stirred a few minutes in the dark, and  $A$  is the characteristic absorbance peak at degradation for a time,  $t$ .

### 3 RESULTS AND DISCUSSION

The Fig. 2 shows XRD patterns of Cu-doped titanate nanotubes obtained at 2 hours (CuNT-2h) and 4 hours (CuNT-4h). It's very difficult to characterize these materials crystallographically, because that the XRD patterns of these nanotubes are low in intensity with broad peaks [1,3,9]. The XRD profile for all as-prepared CuNT samples showed broad peaks at  $2\theta \approx 10^\circ, 24^\circ, 28^\circ, 48^\circ, 62^\circ$ . Many of the proposed titanate or  $\text{TiO}_2$  structures display XRD peaks at very similar  $2\theta$  values making them difficult to distinguish from

one to another. These samples show similar pattern to layered trititanate structure ( $\text{Na}_2\text{Ti}_6\text{O}_{13}$ ). We have not observed peaks related to  $\text{Cu}^{2+}$  species, what suggested that these ions may intercalate and exchange  $\text{Na}^+$  ions between the titanate layers.

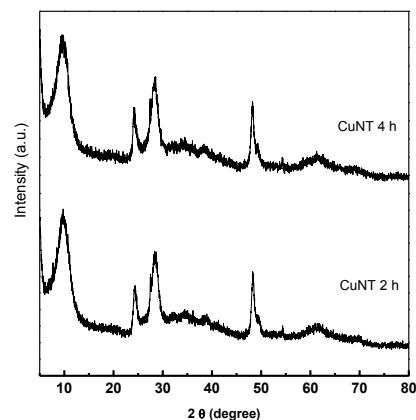


**Figure 2** – XRD patterns titanate nanotubes copper ( $5\%_{\text{wt/wt}}$ ) doped obtained from MWH at  $130^\circ\text{C}$  during 2 and 4 h.

The SEM images of as-synthesized CuNT-2h and CuNT-4h, are showed at Fig. 3, revealed the formation for both samples of well dispersed 1D nanostructures, like nanotubes, with length longer than  $1\ \mu\text{m}$  and width of around  $10\text{ nm}$ . Copper doping of the nanotubes did not dramatically affect their size or morphologie.

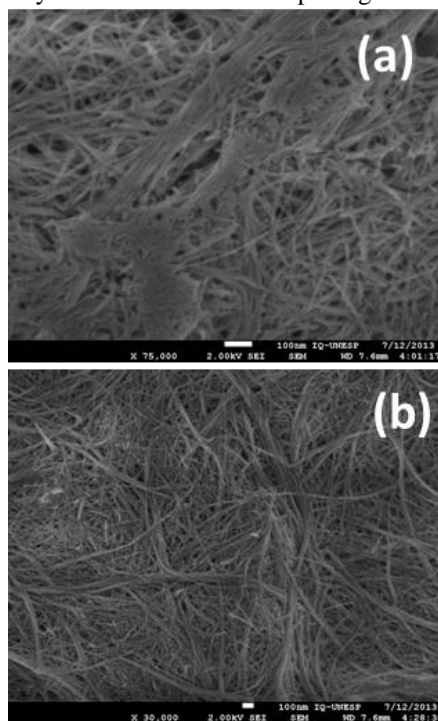


**Figure 3** – SEM images of titanate nanotubes copper ( $5\%$ ) doped obtained from SHM at  $130^\circ\text{C}$  during (a) 2 and (b) 4 h.

The Fig. 4 shows the EDS spectrum from sample CuNT-2h that show the sample composition: sodium, titanium and copper. The peak assigned as Si is related to substrate used in the analysis. The presence of both copper and the sodium on EDS spectrum indicates that these samples were formed by the same mechanism of hydrothermal nanotubes synthesis with the intercalation of  $\text{Na}^+$  with  $\text{Cu}^{2+}$  ions.

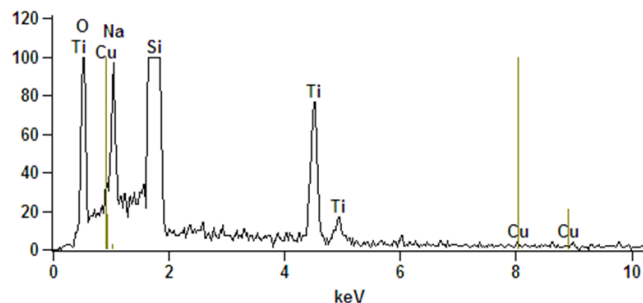


**Figure 4** – EDS spectra for Cu-doped nanotubes obtained from MWH.

The PL emission spectra is useful for investigating intrinsic point defects such as oxygen vacancies. The PL spectra were carried out excited by 350 nm light at room temperature. The original PL spectra and their Gaussian fitting PL peaks for CuNT-2h and CuNT-4h samples are illustrated in Fig. 5.

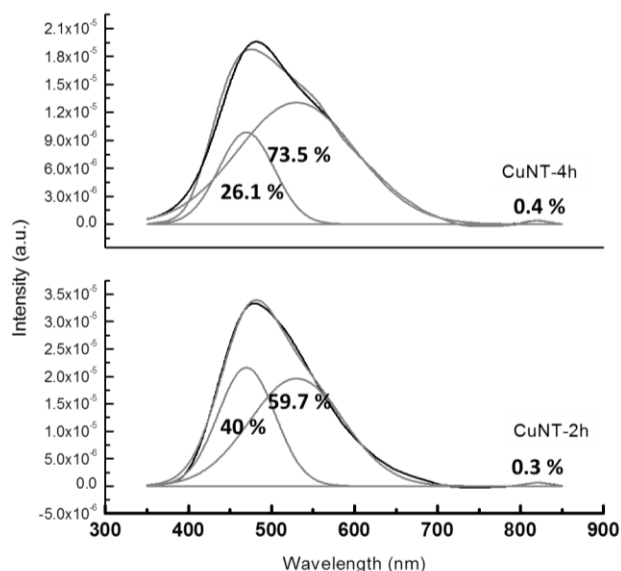


**Figure 5** - PL room temperature spectrum and Gaussian fit bands for the sample CuNT-2h and CuNT-4h (excited at 350 nm).

It can be found that the Gaussian curves fit the original PL curves perfectly. All of the CuNT spectra show that the nanotubes have the main emission bands in the range of 470–480 nm and a relatively broad shoulder. The emission peak present lower intensity for CuNT-4h, indicating the reduction of defects concentration due to longer

hydrothermal treatment duration which promotes the structure organization [ 11, 12].

For sample CuNT-2h we found that the product of deconvolution of spectra gives us bands at the regions blue (470 nm), green (530.5 nm) and a small contribution in the infrared (821 nm) of the spectrum. The most intense contribution is the emission band situated at the green region, approximately corresponding to 59.7%. As well as the band in the blue region of higher energy contributes with 40%. Both are related to the predominance of point defects created during the crystallization process, such as oxygen vacancy and interstitial oxygen. These types of defects insert intermediates energy levels between the conduction band and valence band, which are located closer to the valence band.

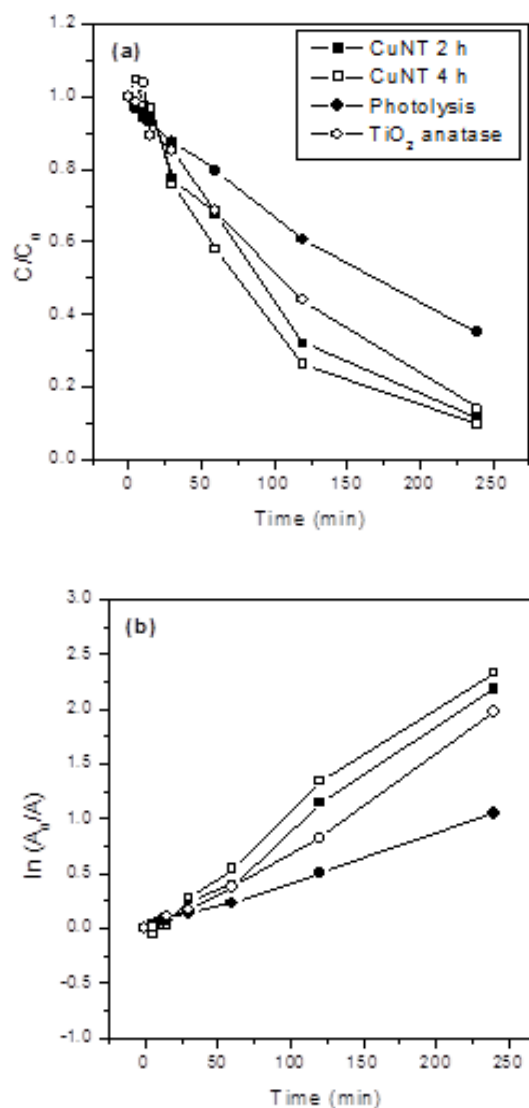
CuNT-4h sample has a slight change on its photoluminescent spectrum, decreasing the emission in blue, to 26.1%, and increasing in the green, up to 73.5%, due the longer hydrothermal synthesis for 4 hours. This shift reveals the injection of charge carriers in the conduction band. The organization of the material, during the hydrothermal treatment, causes decreased energy of the defects, making them increasingly superficial, and inserting shallow levels near the conduction band. Furthermore, it was observed that the photoluminescence emission peak is less intense for the CuNT-4h sample, indicating that the concentration of radiative recombination centers decreases with the increasing on synthesis time, due to a better structural organization.

Fig. 6 shows degradation of RB versus illumination time catalyzed with different samples. Fig. 6.a shows the  $C/C_0$  change with the UV illuminated time. It can be seen that the decolorization efficiency firstly increases for nanotubes copper doped. Table 1 shows a comparison of the rate of discoloration of the samples over time of 120 min and at the end of the experiment (240 min). It appears that at 120 min CuNT-4h has the best performance, reaches 74% of discoloration against 68.1% of the sample CuNT-2h and 57.2%  $\text{TiO}_2$ -anatase. At the end of the experiment, samples CuNT-2h and  $\text{TiO}_2$ -anatase decolorized about 86-88% of the dye while the CuNT-4h reached 99%. This better catalytic performance was ascribed to larger effective contact area between Cu-doped nanotubes and rhodamine b solutions.

Fig 6.b shows the Kinetic study of degradation of RB dye, and the corresponding specific reaction rate constants ( $k$ ) estimated are in Table 1. The reaction rate constants confirm the best photocatalytic activity for the CuNT-4h sample ( $0.01022 \text{ min}^{-1}$ ). Comparing the values of reaction rate constants for photolysis ( $k_{\text{photo}}$ ) with experiments using catalysts, we have that CuNT-4h sample is 2.38 times more efficient than photolysis. Also the CuNT-2h sample was more efficient 2.17 times than photolysis. Finally, we verify that Cu-doped nanotubes are more efficient than  $\text{TiO}_2$ -anatase, precursor used in the MWH.

**Table 1** – Comparison between photocatalytic activities of the samples.

Catalyst	% C/C <sub>0</sub> (120 min)	% C/C <sub>0</sub> (240 min)	k (min <sup>-1</sup> )	k <sub>san</sub> /k <sub>photo</sub>
Photolysis	39.4	65.0	0.00429	1.00
TiO <sub>2</sub>	57.2	86.1	0.00818	1.91
CuNT-2h	68.2	88.8	0.00931	2.17
CuNT-4h	74.0	99.0	0.01022	2.38



**Figure 6** – Photocatalytic studies of TiO<sub>2</sub> anatase and CuNT 2 and 4 hours: a) time dependence and (b) kinetic study of degradation of rhodamine dye in the presence of the samples under UV irradiation.

## 4 CONCLUSIONS

The method employed in this study was effective for the synthesis of Cu-doped titanate nanotubes. Both samples, CuNT-2h and CuNT-4h showed photocatalytic activities for decolorization of rhodamine b dye under UV irradiation. The factors that contribute to the best photocatalytic efficiency of the sample CuNT-4h, may be related to predominance of surface defects, verified by photoluminescence emission in the green, which generate intermediate levels on the band gap, which has lower energy. Moreover the lowest concentration of sites of electron-hole recombination leads to high permanence of the electron in the conduction band and thus the oxidation-reduction reactions of the dye.

## ACKNOWLEDGMENTS

The authors would like to thank FAPESP for financial support CEPID/CDMF FAPESP 2013/07296-2.

## REFERENCES

- [1] T. Kasuga, M. Hiramatsu, A. Hoson, T. Sekino, K. Niihara, *Langmuir*, 1998, 14, 3160.
- [2] T. Kasuga, M. Hiramatsu, A. Hoson, T. Sekino, K. Niihara, *Adv. Mater.* 1999, 11, 1307.
- [3] B.C. Viana, O.P. Ferreira, A.G. Souza Filho, A.A. Hidalgo, J. Mendes Filho, O.L. Alves. *J Nanopart Res*, 13, 3259–3265, 2011.
- [4] D. Liu, T. Liu, C. Lv, W. Zeng. *J Mater Sci: Mater Electron*, 23, 576–581, 2012.
- [5] V. R.-González, S. O.-Alfaro, L.M. L.-Sánchez, S.-W. Lee. *J Mol Catal A-Chem* 353–354, 163–170, 2012.
- [6] C.-C. Chung, T.-W. Chung, T. C.-K. Yang. *Ind. Eng. Chem. Res.* 47, 2301-2307, 2008.
- [7] P. Umek, M. Pregelj, A. Gloter, P. Cevc, Z. Jaglicic, M. Ceh, U. Pirnat, D. Arcon. *J. Phys. Chem. C* 112, 15311–15319, 2008.
- [8] K. Kiatkittipong, J. Scott, R. Amal. *ACS Appl. Mater. Interfaces* 3, 3988–3996, 2011.
- [9] Y.-P. Peng, S.-L. Lo, H.-H. Ou, S.-W. Lai. *J Hazard Mater* 183, 754–758, 2010.
- [10] D. Fang, K. Huang, S. Liu, J. Huang. *J Braz Chem. Soc*, 19, 1059-1064, 2008.
- [11] S. K. S. Patel, N. S. Gajbhiye. *Proc. of SPIE Vol.* 8461 84611T-1.
- [12] G.F. Teixeira, M.A. Zaghete, G. Gasparotto, M.G.S. Costa, J.W.M. Espinosa, E. Longo, J.A. Varela. *J Alloys Comp*, 512, 124–127, 2012.